TITLE: Optimization of the classification process in the zigzag air classifier for obtaining a high protein sunflower meal – Chemometric and CFD approach

AUTHORS: Vojislav Banjac, Lato Pezo, Milada Pezo, Đuro Vukmirović, Dušica Čolović, Aleksandar Fišteš, Radmilo Čolović

NOTICE: This is the author's version of a work that was accepted for publication *Advanced Powder Technology.* Changes resulting from the publishing process, such as peer review, editing, corrections, structural formatting, and other quality control mechanisms may not be reflected in this document. Changes may have been made to this work since it was submitted for publication. A definitive version was subsequently published in *Advanced Powder Technology*, Volume 28, Issue 3, March 2017, Pages 1069–1078. DOI: 10.1016/j.apt.2017.01.013

Optimization of the classification process in the zigzag air classifier for obtaining a high protein sunflower meal - Chemometric and CFD approach

Vojislav Banjac[a,b*], Lato Pezo[c], Milada Pezo[d], Đuro Vukmirović[a], Dušica Čolović[a], Aleksandar Fišteš[b], Radmilo Čolović[a]

[a]*University of Novi Sad, Institute of Food Technology, Bulevar cara Lazara 1, 21000 Novi Sad, Serbia*

[b]*University of Novi Sad, Faculty of Technology, Bulevar cara Lazara 1, 21000 Novi Sad, Serbia*

[c]*University of Belgrade, Institute of General and Physical Chemistry, Studentski Trg 12-16, 11000 Belgrade, Serbia*

[d]*University of Belgrade, Laboratory for Thermal Engineering and Energy, Institute of Nuclear Sciences "Vinča", P.O. Box 522, 11001 Belgrade, Serbia*

[*] Corresponding author. Tel: +381 21 485 3775

E-mail address: vojislav.banjac@fins.uns.ac.rs

E-mail addresses of other authors:

Lato Pezo: latopezo@yahoo.co.uk

Milada Pezo: milada@vinca.rs

Đuro Vukmirović: djuro.vukmirovic@fins.uns.ac.rs

Dušica Čolović: dusica.ivanov@fins.uns.ac.rs

Aleksandar Fišteš: fistes@uns.ac.rs

Radmilo Čolović: radmilo.colovic@fins.uns.ac.rs

Abstract

In this study, sunflower meal is ground by a hammer mill after which air zigzag gravitational air classifier is used for separating sunflower hulls from the kernels in order to obtain protein rich fractions. Three hammer mill sieves with sieve openings diameter of 3, 2 and 1 mm were used, while three air flows (5, 8.7 and 12.5 m^3/h) and three feed rates (30, 60 an 90% of bowl feeder oscillation maximum rate) were varied during air classification process. For describing the effects of the test variables on the observed responses Principal Component Analysis, Standard Score analysis and Response Surface Methodology were used. Beside experimental investigations, CFD model was used for numerical optimization of sunflower meal air classification process.

Air classification of hammer milled sunflower meal resulted in coarse fractions enriched in protein content. The decrease in sieve openings diameter of the hammer mill sieve increased protein content in coarse fractions of sunflower meal obtained at same air flow, and at the same time decreased matching fraction yield. Increase in air flow lead to the increase in protein content along the same hammer mill sieve. Standard score analysis showed that optimum values for protein content and ratio of coarse and fine fractions have been retained by using a sieve with 1 mm opening diameter, air flow of 12.5 m^3/h and 60% of the maximum feeder rate. Fraction ratio and protein content were mostly affected by the linear term of air flow and the sieve openings diameter of the hammer mill sieve in the Second Order Polynomial model. The main focus of CFD analysis was on the particle simulation and the evaluation of the separation efficiency of the zigzag classifier.

Keywords: Sunflower meal; air classification; hammer mill; CFD; optimization

Nomenclature

Symbols		Greek symbols	
BFOR	bowl feeder oscillation rate (% of maximal rate)	γ_F	yield of fine fraction
C	mass of coarse fraction (g)	γ_C	yield of coarse fraction
d	diameter of sieve opening (μm)	κ	separation function
F	mass of fine fraction (g)	Statistical abbreviations	
FR	feed rate of air classifier (kg/h)	ANOVA	analysis of variance
GMD	geometric mean diameter (μm)	PCA	principal component analysis
H_0	hull share in starting sunflower meal	r^2	coefficient of determination
H_C	hull share in coarse fraction	RSM	response surface methodology
H_F	hull share in fine fraction	SOP	second order polynomial
I_0	motor amperage of hammer mill without the material (A)	SD	standard deviation
I	motor amperage of hammer mill with the material (A)	SS	standard score
K_0	kernel share in starting sunflower meal	Abbreviations	

K_C	kernel share in coarse fraction	CFD	computational fluid dynamics
K_F	kernel share in fine fraction	DM	dry matter
P_0	protein content of starting sunflower meal(%DM)	DPM	discrete phase model
P_C	protein content of coarse fraction (%DM)	SFM	sunflower meal
P_F	protein content of fine fraction (%DM)		
Q	material throughput of hammer mill (kg/h)		
R_{fy}	ratio of coarse and fine fraction yield		
SEC	specific energy consumption of hammer mill (kWh/t)		
SOD	sieve openings diameter (mm)		
t	classification time (s)		
U	voltage (V)		
W	mass of the material retained onto sieve (g)		
X	variable		

Y	response		

1. Introduction

Sunflower meal (SFM) is a valuable by-product that remains in large quantities after solvent extraction of oil from sunflower seeds. It is a relatively inexpensive protein and energy source, thus it is primarily used as feed for all classes of animals. Protein content is the most important nutritional component of SFM and it ranges from 29 to 48% [1–3]. Comparing it with other oilseed meals, such as soybean and rapeseed meal, SFM contains less antinutritional factors and it is relatively rich in sulphuric amino acids but has low levels of lysine [4]. SFM has high crude fiber content (18–23%) which is limiting factor in the usage of SFM in diet formulation for monogastric animals. As the protein and fiber content of SFM are inversely related, removal of the fiber rich hulls decreases the fiber and increases the protein content, which improves the nutritive and economic value of it. Additionally, the separation of fibers from SFM would give a coproduct that could be used as fiber rich feed for ruminants or as a combustion fuel.

Various fractionation procedures, based on structural and physical differences of its constituents, such as sieving, centrifugal and electrostatic separation have been used for protein shifting of different plant material [5–8]. Chala et al. [9] have applied air classification process in combination with sieving for fractionation of soybean and cottonseed meal to obtain fiber and protein rich fractions. Wu and Abbott [10] obtained fine fractions of pin milled, defatted salicornia meal using air classification which had 2.9–11% higher protein content than the starting material. In several studies, where air classification was used for obtaining products enriched in specific constituent, it was reported use of high intensity milling process in combination with expensive separators for fine separation [11–15]. As the

protein enriched SFM is used as a feedstuff in animal diets [16–18], there is need of finding low-cost alternatives for improvement of quality and nutritive value of the SFM.

For the purpose of SFM air classification, zigzag air classifier was used in this study. Zigzag air classifier is cascade classifier that consists of vertical zigzag channel where several pipes with rectangular cross section are connected at a fixed angle to each other. A channel that was formed this way enables multi stage classification and therefore improves the separation efficiency [19].

Fines are dragged by the air stream upwards and coarse particles are pulled down by gravity towards the walls of zigzag channel. Due to its simple construction and principle of classification this device has low investment and operational costs. This type of air classifier is widely used in tea in the tobacco industry for separation of leaves from stalks [20] and well as in waste treatment and recycling industry [21]. The authors previously used zigzag air classifier for obtaining protein enriched fractions of conical milled SFM which was coarsely ground on a conical mill [22]. To the best of our knowledge, there are no other works about usage of zigzag air classifier for the increasing nutritive value of oilseed meals or any other raw material.

Phenomenon of particle separation is of great interest of researchers. Fluid–particle and particle–particle interactions play major roles in such systems, which results in the empirical experience more predominant. The prediction of the motion of particles in such systems is very complex due to intense fluid–particle and particle–particle interactions. It can be obtained by numerical simulations of CFD (Computational Fluid Dynamics).

Since classifiers and separators have been used in various industries in the past, a considerable number of investigations on the gas and the particle flows in classifiers have been conducted over the years [23–35].

The geometry of the classifier has great influence on its performances [36,37]. The Reynolds Stress Model and the Discrete Phase Model (DPM) are used to predict the velocity field and pressure drop and to estimate the selectivity curve inside the high-efficiency separator.
The optimization of the cyclone separator for minimal pressure drop using mathematical modeling and CFD simulations was performed in [30]. The Nelder–Mead method, also known as the downhill simplex method is a commonly used nonlinear optimization technique. The technique was proposed by Nelder and Mead [38] and is a technique for minimizing an objective function in a many-dimensional space.
Hagemaier et al. [39] employed one-way coupled CFD-DPM simulation to analyze the separation performance of pilot-scale zigzag classifier for classifying sand. In their study, literature regarding zigzag air classifiers is briefly reviewed.
In this paper SFM is ground by hammer mill and air classified using the zigzag apparatus in order to obtain protein rich fractions. CFD simulation is presented for the pilot scale air classifier. The influence of geometry of the device and the working parameters on separation efficiency is investigated. Experimental results are used for validation of the presented model.

2. Materials and methods

2.1. Raw materials and grinding

SFM, sunflower hull and sunflower kernel, used in this experiment, were obtained from oil factory “Victoria Oil”, Šid, Serbia. Prior the air classification the SFM was ground using a hammer mill (ABC Engineering, Pančevo, Serbia). Different grinding intensity of SFM was obtained by using three different sieves with openings diameters (SOD) of 3, 2 and 1 mm respectively. By measuring the amperage and material throughput, specific energy

consumption (SEC) for grinding was calculated in kWh/t according to equation described by Payne et al. [40]:

$$SEC=\frac{(I-I_0)\cdot U\cdot \cos\varphi\cdot\sqrt{3}}{1000\cdot Q} \quad (1)$$

where I (A) and I_0 (A) are average hammer mill motor amperage with and without material, respectively, U (V) is the voltage, cosφ is the power factor (ratio between the actual load power and the apparent load power drawn by an electrical load) and Q (kg/h) is the throughput of material. Material throughput was influenced by SOD and it was 306.48, 198.20 and 119.08 kg/h for sieve with SOD of 3, 2 and 1 mm respectively.

2.2. Physical characteristics of SFM and obtained SFM fractions

Bulk density (BD) of starting SFM and ground SFMs at all three used sieves was measured with a bulk density tester (Tonindustrie, West und Goslar, Germany). Particle size distribution (PSD) of starting and hammer milled SFMs was determined by standard sieving analysis [41] using the following size of sieve openings: 2500, 2000, 1250, 1000, 800, 630, 250, 125 and 63 μm, along with the bottom collecting pan (Endecotts Ltd., United Kingdom). Geometric mean diameter (GMD) was determined according to ASAE Standard [42] using the equation:

$$GMD= \log^{-1}\left[\frac{\sum_{i=1}^{n}(W_i*\log d_i')}{\sum_{i=1}^{n}W_i}\right] \quad (2)$$

$$d_i'=\sqrt{d_i+d_{i+1}} \quad (3)$$

where d_i (μm) is the diameter of sieve openings of i^{th} sieve and W_i (g) is the mass on i^{th} sieve.

2.3. Air classification

All three ground SFMs were fractionated by an air classification, using 1-40MZM laboratory zigzag air classifier (Hosokawa Alpine, Augsburg, Germany). Air flow and dosage of the material in classification zone were varied. Air flow (V) was set at 5, 8.7 and 12.5 m^3/h, respectively. Material throughput was varied by changing the oscillation rate of the bowl feeder from the controller. Bowl feeder oscillation rate (BFOR) was set at 30%, 60% and 90% of the maximum rate, respectively. Feed rate was determined by measuring the time needed for the classification at each combination of air flow and BFOR. It was calculated as:

$$FR=\frac{C+F}{t}\cdot 3.6 \tag{4}$$

where FR represents feed rate (kg/h), C and F are masses of the obtained coarse and fine fractions respectively (g), and t represents classification time (s). Yields of the obtained fractions were calculated according to equations:

$$\gamma_C=\frac{C}{C+F};\qquad \gamma_F=\frac{F}{C+F};\qquad R_{fy}=\frac{C}{F} \tag{5}$$

where γ_C and γ_F represents a yield of coarse and fine fractions respectively, C mass of coarse fraction (g), F mass of fine fraction (g) and R_{fy} is the mass ratio of coarse and fine fraction yields.

Sunflower hulls were obtained from the same factory, in order to calculate the share of hulls in starting SFM and also in obtained SFM fractions in order to characterize the quality of the

separated products. Assuming that starting SFM and its coarse and fine fractions are a mixture consisting out of two materials, sunflower hulls and kernels, sum of shares of these SFM constituents is 1.

$$H_0+K_0=1;\quad H_C+K_C=1;\quad H_F+K_F=1 \tag{6}$$

H_0 is the share of sunflower hulls in starting SFM, H_C and H_F are shares of sunflower hulls in coarse and fine fraction, respectively. K_0, K_C and K_F are shares of sunflower kernels in starting SFM, coarse and fine SFM fraction, respectively.

Protein content of SFM is directly correlated with a protein content of hull and kernel:

$$H_0\cdot P_h+K_0\cdot P_k=P_0;\ H_C\cdot P_h+K_C\cdot P_k=P_C;\ H_F\cdot P_h+K_F\cdot P_k=P_F \tag{7}$$

P_h, P_k, P_C, P_F and P_0 represent protein content on dry matter basis (%DM) of sunflower hull, kernel, coarse fraction, fine fraction and starting SFM, respectively. By combining Eqns. (6) and (7), hull share in starting SFM, coarse and fine fractions can be calculated by:

$$H_F=\frac{P_k-P_F}{P_k-P_h};\qquad H_C=\frac{P_k-P_C}{P_k-P_h};\qquad H_0=\frac{P_k-P_0}{P_k-P_h} \tag{8}$$

In ideal separation of hull from protein rich kernels, the share of hull in obtained fraction would be 0, and that SFM fraction would have the same content of crude protein as the sunflower kernel, thus protein content of fraction obtained fraction by air classification is directly related to kernel share.

2.4. Chemical analysis

Starting SFM, air classified SFM, sunflower hulls and kernels were analyzed for moisture content and crude protein content. Additionally, unclassified SFM was analyzed for crude fiber content, crude ash and crude fat content. Chemical analysis was performed according to the AOAC official methods [43].

2.5. Experimental design

The experimental data used for the study of experimental results were obtained using 3 x 3 x 3 full factorial experimental design (3 SODs, 3 air flows, 3 BFORs) according to RSM Independent experimental factors are presented in Table 1.

Table 1. Independent experimental factors and their levels

2.6. Description of the CFD model

The model used for these simulations is a Lagrangian discrete phase model based on the Euler-Lagrange approach. The fluid phase is treated as a continuum by solving the Navier-Stokes equations, while the dispersed phase is solved by tracking a large number of particles through the calculated flow field. The dispersed phase can exchange momentum, mass, and energy with the fluid phase. It is assumed that the second phase is sufficiently dilute that particle-particle interactions and the effects of the particle volume fraction on the gas phase are negligible.

A fundamental assumption made in this model is that the dispersed second phase occupies a low volume fraction (usually less than 10–12%, where the volume fraction is the ratio between the total volume of particles and the volume of fluid domain), even though high mass loading is acceptable. The particle trajectories are computed individually at specified

intervals during the fluid phase calculation. This makes the model appropriate for the modeling of particle-laden flows. The particle loading in industrial classifier is small (3–5%), and therefore, it can be safely assumed that the presence of the particles does not affect the flow field (one-way coupling) [30].

In terms of the Eulerian–Lagrangian approach (one- way coupling), the equation of particle motion is given by [44].

The drag coefficient for spherical particles is calculated by using the correlations developed by Morsi and Alexander [45] as a function of the relative Reynolds numbers (Re_p). The equation of motion for particles was integrated along the trajectory of an individual particle. Collection efficiency statistics were obtained by releasing a specified number of mono-dispersed particles at the inlet of the classifier and by monitoring the number escaping through the outlet. Collisions between particles and the walls of the classifier were assumed to be perfectly elastic (coefficient of restitution is equal to 1).

Boundary conditions are defined as follows: inlet – air velocity, two outlets – pressure outlet 100001 Pa and 95000 Pa, inlet – number of particles.

The solid phase is defined by three different feed rates and three diameters, while the fluid phase is introduced at the fluid inlet surface with the three different air flows, corresponding to experimental design described in Table 4. The maximum number of time steps for each injection was 200,000 steps. The numerical experiments are performed for appropriate working conditions.

Numerical grids are made from 109,540 to 111,320 control volumes. Optimization of numerical grid was performed, and grid refinement tests showed that there is no change in the results of the simulation for larger number of cells in control volume. Elements used in numerical mesh are tetrahedral and size of an element is less than 10^{-8} m^3.

2.7. Statistical analyses

The data were processed statistically using the software package STATISTICA 10.0 [46]. All determinations were made in duplicate, all data was averaged, expressed by means. Principal component analysis (PCA) was used to discover the possible correlations among measured parameters, and to classify the objects into groups.

Second order polynomial (SOP) models in the following form were developed to relate responses (Y) and two process variables (X):

$$Y_k=\beta_{k0}+\sum_{i=1}^{2}\beta_{ki}\cdot X_i+\sum_{i=1}^{2}\beta_{kii}\cdot X^2{}_i+\beta_{k12}\cdot X_1\cdot X_2,\ k=1\text{-}2 \quad (9)$$

where: β_{k0}, β_{ki}, β_{kii}, β_{k12} were constant regression coefficients; Y_k : the ratio of fractions gain (Y_1), the protein content of coarse fraction (Y_2), the hull share in the coarse fraction (Y_3), and the kernel share in the coarse fraction (Y_4), while X_1 is the SOD of the hammer mill, X_2 is the air flow and X_3 is the BFOR setting that influenced material flow rate at the inlet of the classifier. In this article, ANOVA was conducted to show the significant effects of independent variables to the responses, and to show which of responses were significantly affected by the varying treatment combinations. For analyzing variations of the SFM properties after grinding, one-way ANOVA and Tukey honestly significant difference test were used (confidence level set at 95%).

In order to get a more complex observation of the ranking of observed model mixtures, standard score (SS) was evaluated using a chemometric approach by experimentally measured responses. Min-max normalization is one of the most widely used technique to compare various characteristics of complex samples determined using multiple measurements, where samples are ranked based on the ratio of raw data and extreme values of the measurement used [47]. The sum of normalized scores of a sample of different

measurements when averaged give a single unitless value termed as SS, which is a specific combination of data from different measuring methods with no unit limitation.

3. Results and Discussion

The drawing of the zigzag classifier, with the control boundary used for numerical simulation of the process is given in Fig. 1a. Fig. 1b - Fig. 1e presents the process of SFM classification. The SFM that is being classified in the classifier is introduced in the material inlet port, while the air, used for separation, enters at the bottom of the classifier.

The zigzag air classifier consists of a number of sections with a rectangular cross section connected to each other at angle of 120^{o}, connected to create a zigzag shaped channel. The heavier (larger and coarser) particles are classified according to their specific weight in the zigzag channel (guided by the influence of the gravitational force) while the air stream is flowing upwards. Coarser, also particles with higher density tends to drop, carried by the gravitational force, while the lighter particles are transported through the upper section of the classifier, at the fine particles outlet. The main air flow stream in the zigzag channel separates from the classifier wall at the protruding edge. At the upper boundary of the observed classifier, the turbulent eddies breaking away from the main air stream was observed, in the direction of air flow. The upper part of the classifier, close to the material inlet is presented in Fig 1b and Fig 1c. A small eddy formation could be observed, indicated as the whiter particle cloud, at the left side, opposite to the material inlet (Fig. 1b). Somewhat larger eddy could be observed in the middle section of the classifier (Fig. 1d), while the particle trajectories could be seen in Fig. 1e.

Figure 1. Zigzag classifier: a) scheme of the classifier used in the numerical model, b) and c) material inlet, d) middle section of the classifier, e) coarse material outlet segment

3.1. SFM properties

Chemical composition of starting SFM is presented in Table 2.

Table 2. Chemical composition of unclassified sunflower meal

Protein content of starting SFM was 32.75%, while the crude fiber content was 19.39 %. The crude fat content was reasonably low (1.94), since the SFM was a byproduct after the oil extraction process. Based on the results of chemical analysis, it was calculated that hulls share in starting SFM was 34.16% and shares of kernel was 65.84%. The reason for the application of air classification on SFM is to remove sunflower hull as a lighter material and fiber rich constituent from kernels, which are heavier and rich in protein. However, during the sunflower oil extraction process, hulls and kernels are forming agglomerates which have the same chemical composition as a SFM in total. During the classification, these agglomerates might finish in the heavier, coarser, fraction which would negatively affect the efficiency of this process. Therefore SFM was ground using a hammer mill prior to the air classification. In Fig. 2, particle size distribution of starting SFM as well SMFs ground by a hammer mill using three sieves with different SOD is presented.

Figure 2. Particle size distribution of starting SFM, and hammer milled SFMs using three sieves with different SOD

More than 50% of the particles of starting SFM were larger than 1250 μm. Due to the presence of agglomerates, originated from the oil extraction process, the highest percent of starting SFM particles were larger than 2500 μm. Application of hammer mill on SFM almost

completely comminuted agglomerates using all three sieves since grinded materials had no particles larger than 2500 μm and negligible percent of particles between 2000 and 2500 μm (Fig. 2). Furthermore, SOD of 2 mm and 1 mm resulted in ground material that had less than 6% for SOD 2 mm, and no particles, for SOD 1 mm larger than 1000 μm. All three sieves with different SOD that were used, gave ground SFM that had most particles in a size range between 250 and 630 μm.

Table 3. Physical properties of starting and hammer milled SFMs

By decreasing SOD, energy consumption of hammer mill was significantly increased (Table 3). This was especially pronounced for diameter of 1 mm where specific energy consumption was 6.57 kWh/t, while energy consumption of hammer mill with SOD of 2 mm was 1.69 kWh/t and use of 3 mm SOD resulted in lowest specific energy consumption that was 0.36 kWh/t. Finer grinding of SFM by a hammer mill exponentially increased specific energy consumption, which is in accordance with the results of Amerah et al. [48] and Vukmirović et al. [49]. Decrease in SOD significantly decreased ($p<0.05$) GMD of SFM, from 1127.36 μm to 573.01 μm, 453.06 μm, and 342.92 μm, for 3, 2 and 1 mm SOD, respectively. By decreasing SOD of hammer mill sieve, bulk density of SFM is significantly increased ($p<0.05$), which is a result of the obtained finer material when sieve with smaller SOD was used. However, the starting SFM had a highest bulk density in comparison with hammer milled SFMs, which was influenced by the presence of large and dense agglomerates.

3.2. Classification results, descriptive statistics, SS and PCA

The results of air classification are presented in Table 4, while for visualizing the data trends and for the discriminating efficiency of the used descriptors a scatter plot of samples using

the first two principal components (PCs) from PCA of the data matrix is obtained (Fig. 3. As can be seen from this figure, there is a neat separation of the twenty seven samples of ground SFM, according to four response variables. The influence of different parameters that describes the observed fractions could be evaluated from the scatter plot. The quality results showed that first two principal components explained 92.55% of total variance, which could be considered as enough for presentation of the whole set of experimental data. Standard score analysis (SS) was used to develop the optimal final product characteristics, and obtained data are presented in Table 4. SS above 0.700 stands for the high standard in desired process parameters (low R_{fy} and high protein content).

Table 4. Results of air classification of SFM ground by hammer mill

Figure 3. Biplot graphic for air separation of the ground sunflower meal by zigzag air classifier: BFOR-bowl feeder oscillation rate; GMD-geometric mean diameter; H_C-hull share in coarse fraction; K_C-kernel share in coarse fraction; P_C-protein content in coarse fraction; R_{fy}-ratio of fractions yield; SOD-sieve openings diameter; SS-standard score; V-air flow

Air classification of SFM at different combinations of air flow and BFOR resulted in coarse and fine fractions that differed in particle size and protein content. Fines were dragged by the air stream while heavier particles, which could not be scavenged by convenient air flow, ended up in coarse fraction. Particle size of coarse fractions was influenced by SOD of hammer mill together with air flow. Decrease in SOD resulted in decrease of GMD of coarse product while an increase in air flow led to the increase of GMD of coarse fraction particles for all three sieves. Coarse fractions, as expected, were enriched in protein content, since sunflower kernels are richer in protein than hulls and have a higher density. This was

opposite with the result of Laudadio et al. [14] where protein content increase was observed in fine fractions when SFM was micronized and air classified by the turbo-classifier with serial assembled cyclone. Micronization results in very fine material, while our attention was only to separate the hulls from the kernels without very intense grinding that would not result in extra fine material, so that the hull can end up in fine, lighter fraction, by usage of zigzag apparatus. Regardless of the hammer mill SOD, air flow of 5 m^3/h was not efficient for obtaining protein rich coarse fractions, and it was too low for the neat separation of fiber and protein rich particles, which can be observed from Fig. 3 where those fractions (low in protein content and in kernel share, with lower SS values) are located at the left side of the graphic. Increase of air flow led to protein enrichment in the coarse fraction of the same set of BFOR at all three used hammer mill sieves. By setting air flow at 8.7 m^3/h and using hammer mill ground SFM with 3 mm SOD, protein content of coarse fraction slightly increased when compared to unclassified SFM, regardless of the BFOR (protein content was in the range 36.01–36.43% on DM basis). Further decreasing of the SOD for same air flow caused an increase of protein content of coarse fractions. The highest protein enrichment effects of air flow set at 8.7 m^3/h were achieved when 1 mm SOD sieve was used for grinding SFM, with obtained fractions that had 42.97%, 43.48% and 41.23 % on DM basis for BFOR setting of 30, 60 and 90 %, respectively.

Applying air flow of 12.5 m^3/h resulted in coarse SFM fractions with highest protein enrichment, when compared to 5 m^3/h and 8.7 m^3/h air flows. The fractions obtained by highest air flow are located at the right side of the PCA graphic (Fig. 3). Likewise with 8.7 m^3/h air flow, decrease in SOD caused an increase in protein content of coarse fraction. Decrease in SOD from 3 to 2 mm led to a slight decrease in protein content of coarse fraction for same BFOR, while for SOD of 1 mm coarse fractions with high protein content of 50.9, 50.88 and 49.46 % per DM were obtained for BFOR set at 30, 60 and 90%, respectively. At

the upper part of PCA graphic fractions of SFM grinded by a hammer mill with largest used SOD (3mm) are located, while the SFM fractions grinded by a hammer mill with the lowest SOD (1 mm) are located at the bottom part of the graphic.

Unlike for the variation of air flow, protein content of coarse fractions when BFOR was varied, and for the same SOD and air flow, were not differing more than 2% on DM basis. When expressing increase in protein content of coarse fraction as a relative enrichment, the highest relative enrichment obtained for 8.7 m^3/h air flow was 20.81% (fraction no. 23 - 1 mm SOD, 60% BFOR, protein content of 43.48% per DM), while the highest relative enrichment obtained for 12.5 m^3/h air flow was 41.43% (fraction no. 21 - 1 mm SOD, 30% BFOR, protein content of 50.90% per DM). Experimentally obtained fraction no. 21, together with fraction no. 24 (1 mm SOD, 12.5 m^3/h, 60% BFOR, protein content of 50.88% per DM), concerned to have optimum values of protein content, kernel and hull share, based on SS analysis. Laudadio et al. [14] have also used air classification for protein enrichment of SFM. The highest protein content they have obtained was 40% on DM basis with 20.12% relative protein enrichment. Challa et al. [9] applied combination of sieving and air classification for protein enrichment of soybean meal and cottonseed meal, which resulted in relative protein enrichment of 6.86 and 9.76%, respectively. Based on protein content in obtained fractions, results in this study gained scientific as well as practical significance.

Variation in air flow and SOD of hammer mill, highly influenced not just the protein content of fractions, but also the ratio of fraction yields (R_{fy}). With the increase in airflow, R_{fy} decreased in all three applied SODs. Also, for constant BFOR and air flow, R_{fy} decreased with the decrease of SOD. Therefore, it can be considered that the R_{fy} was inversely related to the protein content of coarse fraction.

Since the SFM kernel and hull content are inversely related, higher protein content in coarse fraction was a consequence of higher kernel and lower hull share. The same can be concluded

from PCA plot (Fig. 3). Therefore, the highest kernel shares in coarse fraction were obtained for air flow of 12.5 m^3/h and 1 mm SOD: shares of 97.65, 97.61 and 94.59% for BFOR set at 30, 60 and 90%, respectively. These fractions are on the far right end of PCA plot, marked as fraction 21, 24 and 27, respectively. Since the kernels are a constituent of SFM high in protein, to obtain nutritionally more valuable ingredient, their share should be as high as possible. On the other hand, coarse fraction which had the lowest kernel content (60.22%) and the highest hull share (33.36% per DM) was obtained for classification of SFM that was ground by 3 mm SOD sieve, obtained at 5 m^3/h with BFOR set at 90% (protein content of 33.36% per DM), which can be seen at far left end of PC1 (fraction no. 7).

3.3. Response surface methodology

ANOVA exhibits the significant independent variables as well as the interactions of these variables. The analysis revealed that the quadratic terms of SOP model (Eq. (9)) was found significant in all three models calculations. The ANOVA test shows the significant effects of the independent variables to the responses and which of responses were significantly affected by the varying treatment combinations (Table 5). Fraction ratio and protein content were mostly affected by the linear term of air flow and the SOD of hammer mill, and also the nonlinear term SOD × Air flow in the SOP models ($p<0.01$ level). The calculation of fraction ratio was influenced by the quadratic term of air flow, the linear term of BFOR and the nonlinear term of Air flow × BFOR, while the prediction of protein content was affected by the quadratic term of SOD, statistically significant at $p<0.01$ level.

Table 5. ANOVA of sunflower meal classification

The average error between the predicted values and experimental values were below 10%. Values of average error below 10% indicate an adequate fit for practical purposes. To verify the significance of the models, analysis of variance was conducted and the results indicate that all models were significant with minor lack of fit, suggesting they adequately represented the relationship between responses and factors.

All SOP models had an insignificant lack of fit tests, which means that all the models represented the data satisfactorily. A high r^2 is indicative that the variation was accounted and that the data fitted satisfactorily to the proposed model (SOP in this case). The r^2 values for fraction ratio and protein share (0.980 and 0.955, respectively), were found very satisfactory and showed the good fit of the model to experimental results.

3.4. CFD model

The results of numerical simulation for optimal case are presented in Fig. 4. The main focus in this simulation was the discovery of the particle trajectory and the evaluation of the separation efficiency of the zigzag apparatus. The numerical simulations of 27 cases of air classification were performed, according to experimental design, shown in Table 4. The trajectory of fifteen representative kernel particles obtained from the DPM simulations of the optimal case, are shown in Fig. 4a. Similarly, the trajectory of 15 representative hull particles, calculated in DPM simulations of the optimal case are presented in Fig. 4b. The effects of the end-of-the-vortex phenomenon are due to two possible stable positions of the vortex core depending on the inlet flow rate [50].

According to DPM simulations, presented in Fig. 4a and Fig. 4b, the particles enter the classifier from the material inlet, and heavier particles (kernels) fall down to the bottom outlet of zigzag classifier, driven by the gravitational force. A small eddy could be observed in the first separation section, where the classifying of different particles is obtained by the action of

air flow (which could be also observed in Fig. 1b). The lighter particles are transported from the material inlet to the upper outlet of the separator, carried by the air flow. In this case, the force applied by the airflow, prevails the gravitational force, due to a relatively small hull weight (Fig. 4b). The pressure field of the fluid phase (air) along the whole classifier is shown in Fig. 4c, from which it could be seen that the higher pressure values could be expected at the lower part of the separator (where the air inlet is positioned), while the lower pressure values could be observed at the upper part of the separator, where the air outlet is located. The variations in the pressure values also occur due to the geometrical features of the classifier, at the protruding edges and air flow gaps, where the eddies could be formed.

Figure 4. The results of the CFD model: a) upper and central parts of the classifier, with particle trajectories of kernel share, b) upper segment of the classifier, with particle trajectories for hull share, c) pressure field in the fluid phase (Pa)

The separation function describes the particle separation quality of the classification process. In general, it is defined as the ratio of the mass flow rate of the coarse product in the separator underflow to the mass flow rate of the feed (κ=K_c/H_c in CFD simulation). The calculated values obtained from CFD simulation, are presented in Table 4. The separation efficiency values, which were obtained by CFD simulation coincide with the experimental results of air classification. The deviations between experimental and numerical separation function were in the area of 10–20%, for a specific experiment. The parameters used in CFD model are for ideal working conditions, and deviation in the obtained area (10–20%) could be considered as acceptable [50].

4. Conclusions

Grinding of SFM by hammer mill in combination with the air classification using zigzag classifier resulted in coarse fractions with enriched protein content. The increase in airflow increased protein content in the coarse fraction for all three used SODs of hammer mill sieve, fraction yield was decreased. Decrease in SOD lead to the increase in protein content of coarse fraction. Standard score analysis showed that the best result in protein enrichment of SFM was obtained by grinding with 1 mm SOD and using air flow of 12.5 m^3/h, where coarse fractions had a protein content of 50.90, 50.88 and 49.86% on DM basis obtained at BFOR of 30, 60 and 90 %, respectively. Kernel share in coarse fractions was in direct correlation with the protein content of coarse fraction. Experimental results of air classification were confirmed by separation efficiency values obtained by CFD simulation. The deviations between experimental and separation function obtained by the numerical simulations were in the area of 10–20%, for a specific experiment.

5. Acknowledgments

This work is a part of Integrated and Interdisciplinary Research Project No III 46012, funded by the Ministry of Education, Science and Technological development of the Republic of Serbia.

6. References

[1] R. Boni, A. Assogna, F. Grillo, A. Robertiello, F. Petrucci, E. Giacomozzi, A. Patricelli, European Patent EP0 271 964 A2, 1987.

[2] S. Ramachandran, S.K.Singh, C. Larroche, C.R. Soccol, A. Pandey, Oil cakes and their biotechnological applications: a review, Bioresource Technology, 98 (2007) 2000 - 2009.

[3] C. Geneau-Sbartaï, J. Leyris, F. Silvestre, L. Rigal, Sunflower cake as a natural composite: composition and plastic properties, Journal of Agricultural Food Chemistry, 56 (2008) 11198 - 11208.

[4] S.N. Mérida, A. Tomás-Vidal, S. Martínez-Llorens, M.J. Cerdá, Sunflower meal as a partial substitute in juvenile sharpsnout sea bream (*Diploduspuntazzo*) diets: Amino acid retention, gut and liver histology, Aquaculture, 298 (2010) 275 - 281.

[5] S. Sredanović, Advancement of technological process and quality of sunflower meal (MSc thesis) University of Novi Sad, Faculty of Technology, 2007.

[6] R. Srinivisan, F. To, E. Columbus, Pilot scale fiber separation from distillers dried grains with solubles using sieving and air classification, Bioresource Technology, 100 (2009) 3548 - 3555.

[7] T.S. Pandya, R. Srinivisan, Effect of hammer mill retention screen size on fiber separation from corn flour using the Elusive process, Industrial Crops and Products, 35 (2012) 37 - 43.

[8] J. Wang, J. Zhao, M. de Wit, R.M. Boom, A.I. Schutyser, Lupine proteine concentrate enrichment by milling and electrosatic separation, Innovative Food Science and Emerging Technologies, 33 (2016) 596 - 602.

[9] R. Challa, R. Srinivasan, F. To, Fractionation of soybean meal, cottonseed meal and wheat middlings using combination of sieving and air classification, Animal Feed Science and Technology, 159 (2010) 72 - 78.

[10] V. Wu, T. Abbott, Protein enrichment of defatted salicornia meal by air classification, Journal of the American Oil Chemist's Society, 80 (2003) 167 - 169.

[11] V. Wu, N. Nichols, Fine grinding and air classification of field pea, Cereal Chemistry, 82 (2005) 341 - 344.

[12] D.G. Stevenson, F.J. Eller, J.-L. Jane, G.E. Inglett, Structure and physicochemical properties of deffated and pin-milled oat bran concentrate fractions separated by air-classification, International Journal of Food Science and Technology, 43 (2008) 995 - 1003.

[13] B. Ferrari, F. Finocchiaro, A.M. Stanca, A. Gianinetti, Optimization of air classification for the production of β-glucan-enriched barley flours, Journal of Cereal Science, 50 (2009) 152 - 158.

[14] V. Laudadio, E. Bastoni, M. Introna, V. Tufarelli, Production of low-fiber sunflower (*Helianthus annuss* L.) meal by micronization and air-classification processes, CyTA-Journal of Food, 11 (2013) 398 - 403.

[15] P.J.M. Pelgrom, J. Wang, R.M. Boom, M.A.I. Schutyser, Pre- and post-treatment enhance the protein enrichment from milling and air classification of legumes, Journal of Food Engineering, 155 (2015) 53 - 61.

[16] N. Gill, D.A. Higgs, B.J. Skura, M. Rowshadeli, B. Dosanjh, J. Mann, A.L. Gannam, Nutritive value of partially dehulled and extruded sunflower meal for post-smolt Atlantic salmon (*Salmosalar* L.) in sea water, Aquaculture Research, 37 (2006) 1348 - 1359.

[17] V. Laudadio, E. Ceci, S.H. Nahashon, M. Introna, M., N.M.B. Lastela, V. Tufarellli Influence of substituting dietary soybean for air-classified sunflower (*Heliaunthus annuus* L.) meal on egg production and steroid hormones in early-phase laying hens, Reproduction in Domestic animals, 49 (2014) 158 - 163.

[18] V. Laudadio, M. Introna, N.M.B. Lastella, V. Tufarelli, Feeding of low-fibre sunflower (*Heliaunthus annuus* L.) meal as substitute of soybean meal in turkey rations: Effects on growth performance and meat quality, The Journal of Poultry Science, 51 (2014) 185 - 190.

[19] M. Shapiro, V. Galperin, Air classification of solid particles: a review, Chemical Engineering and Processing, 44 (2005) 279 - 285.

[20] B. Furchner, S. Zampini, Air classifying, in: Ullmann's Encyclopedia of Industrial Chemistry, Volume 2, Wiley-VCH, Weinheim, 2012, pp. 215-234.

[21] T. Friedländer, H.Z. Kuyumcu, L. Rolf, Untersuchung zur Sortierung von PET-Flakes nach der Teilchenform, Aufbereitungstechnik, 47(8/9) (2006) 24 - 28.

[22] V. Banjac, R. Čolović, Đ. Vukmirović, S. Sredanović, D. Čolović, J. Lević, S. Teodosin, Protein enrichment of sunflower meal by air classification. Food & Feed Research, 40 (2013) 77 - 83.

[23] J.C. Cullivan, R.A. Williams, C.R. Cross, Understanding the Hydrocyclone Separator Through Computational Fluid Dynamics**,** Chemical Engineering Research and Design, 81 (2003), 455 - 466.

[24] J. Jiao, Y. Zheng, G. Sun, Numerical simulation of fine particle separation in a rotational tube separator**,** China Particuology, 3 (2005) 219 - 223.

[25] J.P. Veerapen, B.J. Lowry, M.F. Couturier, Design methodology for the swirl separator, Aquacultural Engineering, 33 (2005) 21 - 45.

[26] J.J. Derksen, S. Sundaresan, H.E.A. van den Akker, Simulation of mass-loading effects in gas–solid cyclone separators, Powder Technology, 163 (2006) 59 - 68.

[27] B. Wang, D.L. Xu, K.W. Chu, A.B. Yu, Numerical study of gas–solid flow in a cyclone separator, Applied Mathematical Modelling, 30 (2006) 1326 - 1342.

[28] C. Corte´s, A. Gil, Modeling the gas and particle flow inside cyclone separators, Progress in Energy and Combustion Science, 33 (2007) 409 - 452.

[29] C. Bhasker, Flow simulation in industrial cyclone separator, Advances in Engineering Software, 41 (2010) 220 - 228.

[30] K. Elsayed, C. Lacor, Optimization of the cyclone separator geometry for minimum pressure drop using mathematical models and CFD simulations, Chemical Engineering Science, 65 (2010) 6048 - 6058.

[31] H. Safikhani, M.A. Akhavan-Behabadi, M. Shams, M.H. Rahimyan, Numerical simulation of flow field in three types of standard cyclone separators, Advanced Powder Technology, 21 (2010) 435 - 442.

[32] Y. He, C. Duan, H. Wang, Y. Zhao, D. Tao, Separation of metal laden waste using pulsating air dry material separator, International Journal of Environmental Science & Technology, 8(1) (2011) 73 - 82.

[33] F.J. de Souza, R.V. Salvo, D.A.M. Martins, Large eddy simulation of the gas–particle flow in cyclone separators, Separation and Purification Technology, 94 (2012) 61 - 70.

[34] J. Oh, S. Choi, J. Kim, J. Numerical simulation of an internal flow field in a uniflow cyclone separator, Powder Technology, 274 (2015) 135 - 145.

[35] C. Duan, H. Li, J. He, Y. Zhao, L. Dong, K. Lv, Y. He, Experimental and Numerical Simulation of Spent Catalyst Separation in an Active Pulsing Air Classifier, Separation Science and Technology, 50(5) (2015) 633 - 645.

[36] G. Gong, Z. Yang, S. Zhu, Numerical investigation of the effect of helix angle and leaf margin on the flow pattern and the performance of the axial flow cyclone separator, Applied Mathematical Modelling, 36 (2012) 3916 - 3930.

[37] R. Guizani, I. Mokni, H. Mhiri, P. Bournot, CFD modeling and analysis of the fish-hook effect on the rotor separator's efficiency, Powder Technology, 264 (2014) 149 - 157.

[38] J.A. Nelder, R. Mead, A simplex method for function minimization, The Computer Journal, 7 (1965) 308 - 313.

[39] T. Hagemeier, H. Glöckner, C. Roloff, D. Thévenin, J. Tomas, Simulation of multi-stage particle classification in a zigzag apparatus, Chemical Engineering and Technology, 37 (2014) 879 - 887.

[40] J. Payne, W. Rattink, T. Smith, T. Winowiski, Objectives in pelleting, in: J. Payne, W. Rattink, T. Smith, T. Winowiski (Eds.), The Pelleting Handbook, Borregaard Lignotech, Norway, pp. 11-12.

[41] ISO 2591-1:1988, "Test sieving-Part 1: Methods using test sieves of woven wire cloth and perforated metal plate."

[42] ASAE Methods of Determining and Expressing Fineness of Feed Materials by Sieving,Standard no. S319.3, American Society of Agricultural and Biological Engineers (2003). pp. 202-205.

[43] Association of Analytical Communities (A.O.A.C.), Official Methods of Analysis (16th ed.) (1998) Gaithersburg, MD, USA.

[44] B. Zhao, Y. Su, J. Zhang, Simulation of gas flow pattern and separation efficiency in cyclone with conventional single and spiral double inlet configuration, Chemical Engineering Research and Design, 84 (2006) 1158 - 1165.

[45] S.A. Morsi, A.J. Alexander, An investigation of particle trajectories in two- phase flow systems, Journal of Fluid Mechanics, 55 (1972) 193 - 208.

[46] Stat-Soft Inc, STATISTICA (Data Analysis Software System), version 10.0, 2010, (Tulsa, Ok, USA).

[47] T. Brlek, L. Pezo, N. Voća, T. Krička, Đ. Vukmirović, R. Čolović, M. Bodroža-Solarov, Chemometric approach for assessing the quality of olive cake pellets, Fuel Processing Technology, 116 (2013) 250 - 256.

[48] A.M. Amerah, V. Ravindran, R.G. Lentle, D.G., Thomas, Influence of feed particle size and feed form on the performance, energy utilization, digestive tract development, and digesta parameters of broiler starters, Poultry Science, 86 (2007) 2615 - 2623.

[49] D. Vukmirović, A. Fišteš, J. Lević, R. Čolović, D. Rakić, T. Brlek, V. Banjac, Possibilities for preservation of coarse particles in pelleting process to improve feed quality characteristics. Journal of Animal Physiology and Animal Nutrition, In Press (2016).

[50] G.I. Pisarev, A.C. Hoffmann, Effect of the ‘end of the vortex’ phenomenon on the particle motion and separation in a swirl tube separator, Powder Technology, 222 (2012) 101-107.

Table 1. Independent experimental factors and their levels

		Coded factor's level		
		-1	0	+1
Experimental factor	Symbol	(low)	(centre)	(high)
SOD (mm)	X_1	1	2	3
V (m^3/h)	X_2	5	8.7	12.5
BFOR (% of maximum)	X_3	30	60	90

SOD - sieve opening diameter; V-air flow; BFOR - bowl feeder oscillation rate

Table 2. Chemical composition of unclassified sunflower meal

Chemical composition	**(%)**
Moisture	9.02
Crude protein	35.99*
Crude fiber	19.39*
Crude fat	2.13*
Crude ash	6.75*
Nitrogen free extracts (NFE)	35.73*

* expressed on a dry matter basis

Table 3. Physical properties of starting and hammer milled SFMs

SOD (mm)	SEC (kWh/t)	GMD (μm)	BD (kg/m^3)
Starting SFM	-	1127.36 ± 55.62^d	490 ± 0.00^d
3	0.36 ± 0.01^c	573.01 ± 11.52^c	433 ± 5.77^a
2	1.69 ± 0.03^b	453.06 ± 4.92^b	470 ± 0.00^b
1	6.57 ± 0.20^a	342.92 ± 0.65^a	480 ± 0.00^c

SOD-sieve opening diameter; SEC-specific energy consumption; GMD-Geometric mean diameter; BD-bulk density

*The results are shown as mean value ± standard deviation (n=3); values with different letters in the same column are significantly different ($p<0.05$)

Table 4. Results of air classification of SFM ground by hammer mill

No. of fraction	SOD (mm)	V (m^3/h)	BFOR (% of maximum)	R_{fy}	GMD of coarse fraction (μm)	P_c (%DM)	K_c (%)	H_c (%)	κ	SS
1	3	5	30	4.78	678.40	35.08	63.89	36.11	1.47	0.252
2	3	8.7	30	1.72	769.51	36.19	66.25	33.75	1.64	0.478
3	3	12.5	30	0.40	984.31	43.25	81.33	18.67	3.70	0.764
4	3	5	60	5.84	709.16	36.49	66.90	33.10	1.69	0.225
5	3	8.7	60	1.74	782.70	36.43	66.78	33.22	1.69	0.484
6	3	12.5	60	0.45	1028.92	42.28	79.25	20.75	3.23	0.733
7	3	5	90	7.98	665.79	33.36	60.22	39.78	1.27	0.000
8	3	8.7	90	2.00	787.01	36.01	65.86	34.14	1.59	0.455

9	3	12.5	90	0.52	963.63	41.49	77.56	22.44	2.86	0.706
10	2	5	30	3.75	570.47	36.66	67.26	32.74	1.69	0.363
11	2	8.7	30	1.00	651.93	36.49	66.90	33.10	1.67	0.533
12	2	12.5	30	0.31	792.92	42.50	79.72	20.28	3.23	0.748
13	2	5	60	4.26	558.83	34.28	62.17	37.83	1.35	0.263
14	2	8.7	60	1.08	658.72	38.00	70.12	29.88	1.96	0.571
15	2	12.5	60	0.33	802.26	41.85	78.33	21.67	3.03	0.728
16	2	5	90	5.50	536.66	34.24	62.10	37.90	1.37	0.183
17	2	8.7	90	1.20	648.52	36.74	67.44	32.56	1.72	0.527
18	2	12.5	90	0.31	801.38	41.73	78.08	21.92	2.94	0.726
19	1	5	30	1.75	431.32	35.88	65.60	34.40	1.59	0.468
20	1	8.7	30	0.49	481.62	42.97	80.73	19.27	3.45	0.750
21	1	12.5	30	0.13	575.01	50.90	97.65	2.35	33.33	0.999
22	1	5	60	2.24	420.46	35.78	65.38	34.62	1.59	0.434
23	1	8.7	60	0.51	487.66	43.48	81.82	18.18	3.70	0.763
24	1	12.5	60	0.12	598.77	50.88	97.61	2.39	33.33	0.999
25	1	5	90	3.08	398.59	36.64	67.22	32.78	1.72	0.405
26	1	8.7	90	0.55	476.08	41.23	77.01	22.99	2.78	0.696
27	1	12.5	90	0.11	595.64	49.46	94.59	5.41	14.29	0.959

SOD-sieve openings diameter; V-air flow, BFOR-bowl feeder oscillation rate; R_{fy}-ratio of fractions yield; GMD-geometric mean diameter; P_C-protein content in coarse fraction; Kc-kernel share in coarse fraction; H_C-hull share in coarse fraction; κ-separation function (K_c/H_c in CFD simulation), obtained by CFD model; SS-standard score

Table 5. ANOVA of sunflower meal classification

	df	R_{fy}	P_C
SOD	1	14.905^{+}	121.566^{+}
SOD^2	1	0.021	$33 .955^{+}$
V	1	74.014^{+}	410.220^{+}
V^2	1	8.773^{+}	13.028^{*}
BFOR	1	2.629^{+}	4.524
$BFOR^2$	1	0.110	1.221
SOD × V	1	9.185^{+}	36.063^{+}
SOD × BFOR	1	0.414^{**}	0.128
V × BFOR	1	3.158^{+}	0.031
Error	17	2.324	28.978
r^2		0.980	0.955

R_{fy} -ratio of coarse and fine fraction's yields; P_C-protein content in coarse fraction; SOD-sieve opening diameter; BFOR-bowl feeder oscillation rate; df- degrees of freedom; r^2-coefficient of determination; V-air flow

+Significant at p<0.01 level, *Significant at p<0.05 level, **Significant at p<0.10 level, 95%

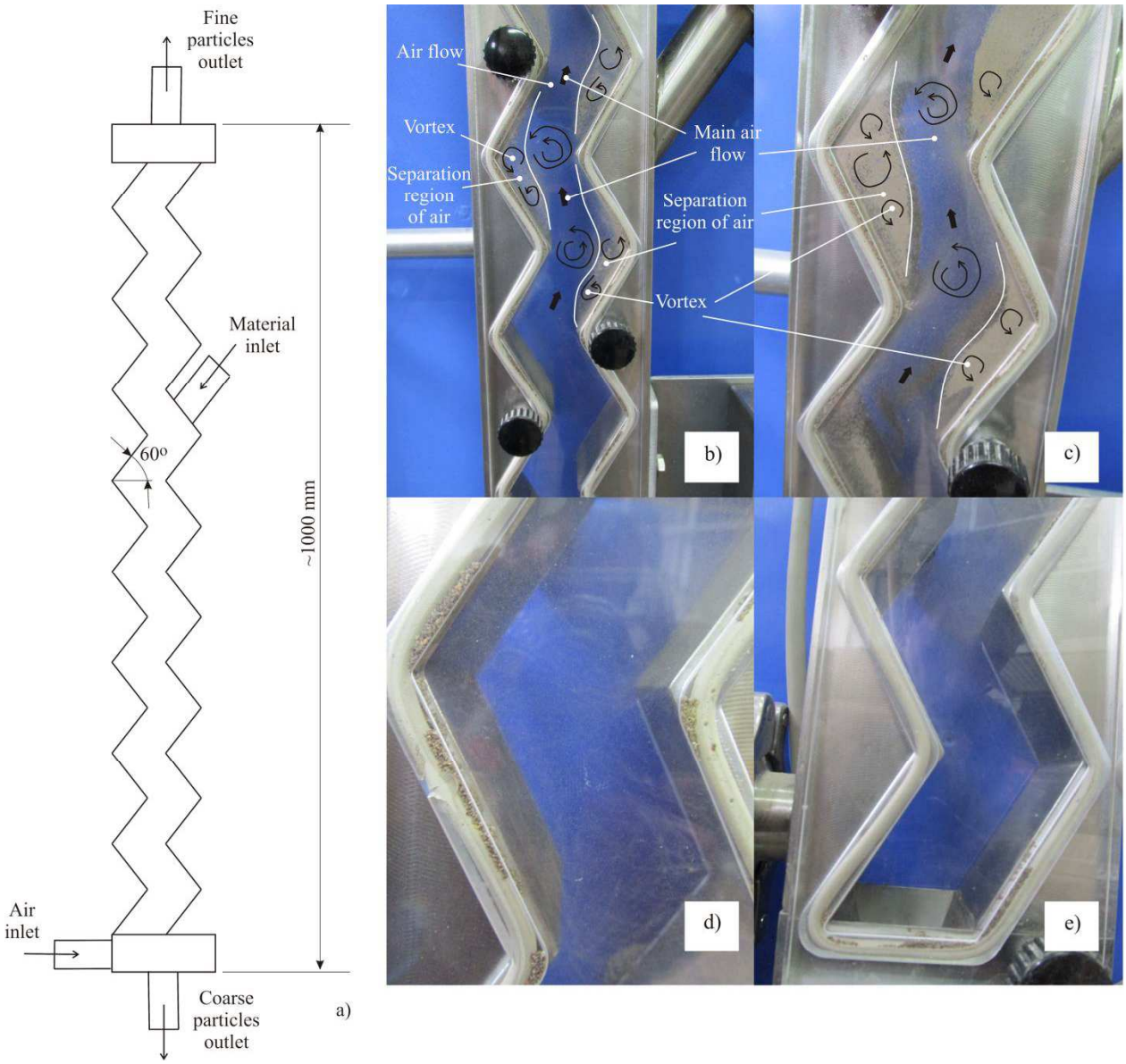

Figure 1. Zigzag classifier: a) scheme of the classifier used in the numerical model, b) and c) material inlet, d) middle section of the classifier, e) coarse material outlet segment

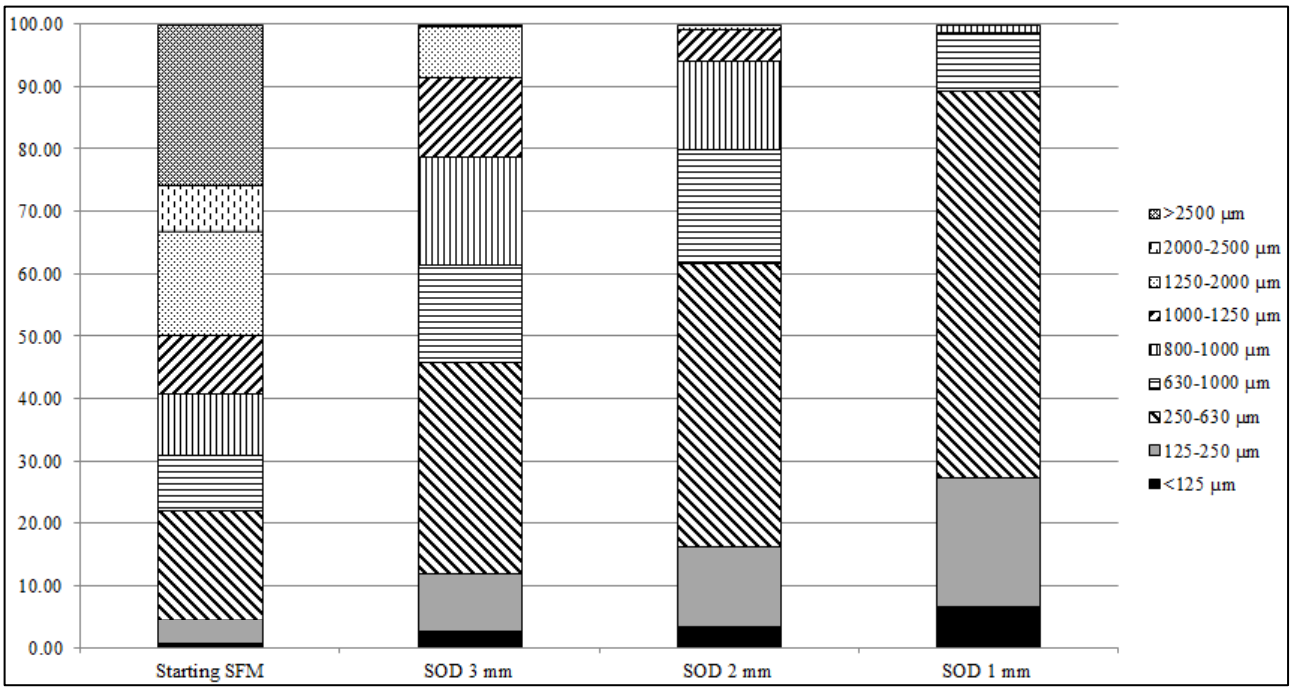

Figure 2. Particle size distribution of starting SFM, and hammer milled SFMs using three sieves with different SOD

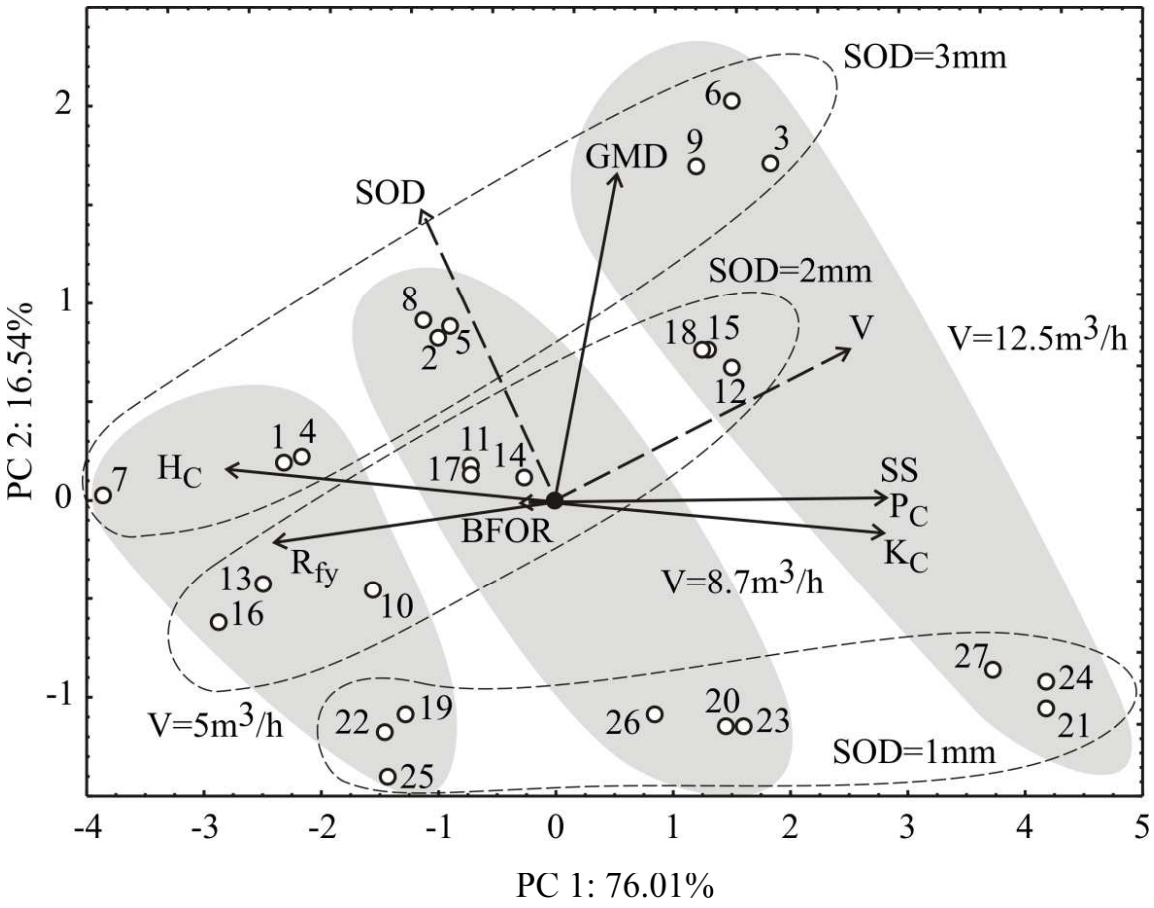

Figure 3. Biplot graphic for air separation of the ground sunflower meal by zigzag air classifier: BFOR-bowl feeder oscillation rate; GMD-geometric mean diameter; H_C-hull share in coarse fraction; K_C-kernel share in coarse fraction; P_C-protein content in coarse fraction; R_{fy}-ratio of fractions yield; SOD-sieve openings diameter; SS-standard score; V-air flow

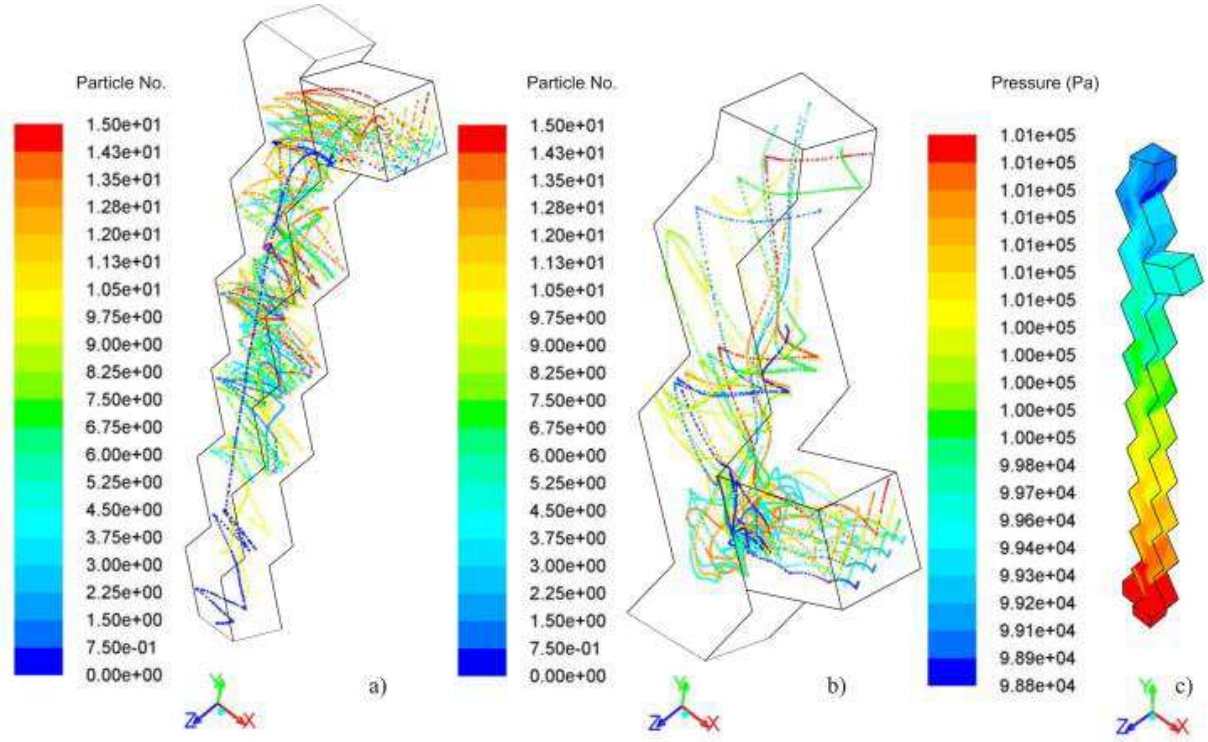

Figure 4. The results of the CFD model: a) upper and central parts of the classifier, with particle trajectories of kernel share, b) upper segment of the classifier, with particle trajectories for hull share, c) pressure field in the fluid phase (Pa)